Cell

Dynamic Interaction between Sigma-1 Receptor and Kv1.2 Shapes Neuronal and Behavioral Responses to Cocaine

Saïd Kourrich,[1] Teruo Hayashi,[2,3,6] Jian-Ying Chuang,[3,6] Shang-Yi Tsai,[3] Tsung-Ping Su,[3] and Antonello Bonci[1,4,5,*]
[1]Cellular Neurobiology Branch
[2]Cellular Stress Signaling Unit
[3]Cellular Pathobiology Section
Intramural Research Program, National Institute on Drug Abuse, Baltimore, MD 21224, USA
[4]Department of Neurology, University of California, San Francisco, San Francisco, CA 94608, USA
[5]Solomon H. Snyder Neuroscience Institute, Johns Hopkins University School of Medicine, Baltimore, MD 21205, USA
[6]These authors contributed equally to this work
*Correspondence: antonello.bonci@nih.gov
http://dx.doi.org/10.1016/j.cell.2012.12.004

SUMMARY

The sigma-1 receptor (Sig-1R), an endoplasmic reticulum (ER) chaperone protein, is an interorganelle signaling modulator that potentially plays a role in drug-seeking behaviors. However, the brain site of action and underlying cellular mechanisms remain unidentified. We found that cocaine exposure triggers a Sig-1R-dependent upregulation of D-type K^+ current in the nucleus accumbens (NAc) that results in neuronal hypoactivity and thereby enhances behavioral cocaine response. Combining ex vivo and in vitro studies, we demonstrated that this neuroadaptation is caused by a persistent protein-protein association between Sig-1Rs and Kv1.2 channels, a phenomenon that is associated to a redistribution of both proteins from intracellular compartments to the plasma membrane. In conclusion, the dynamic Sig-1R-Kv1.2 complex represents a mechanism that shapes neuronal and behavioral response to cocaine. Functional consequences of Sig-1R binding to K^+ channels may have implications for other chronic diseases where maladaptive intrinsic plasticity and Sig-1Rs are engaged.

INTRODUCTION

The sigma-1 receptor (Sig-1R) is a chaperone protein residing at the interface between the endoplasmic reticulum (ER) and the mitochondrion (mitochondrion-associated ER membrane [MAM]) (Hayashi and Su, 2007) that is ubiquitously expressed throughout the brain (Gundlach et al., 1986). Upon ligand stimulation the Sig-1R translocates from the MAM to the ER and plasmalemma (Hayashi and Su, 2003). Acting as an interorganelle signaling modulator, it regulates a variety of functional proteins (Su et al., 2010) either directly or indirectly through G protein-dependent, as well as protein kinase C (PKC)-dependent and protein kinase A (PKA)-dependent signaling pathways (Maurice and Su, 2009). In addition, in vitro activation of the Sig-1R increases (Soriani et al., 1998) or decreases (Zhang and Cuevas, 2005) neuronal excitability through changes in voltage-gated K^+ currents (Kourrich et al., 2012b). Whether these changes occur through G protein-dependent signaling pathways (He et al., 2012; Soriani et al., 1998) remains controversial (Lupardus et al., 2000; Zhang and Cuevas, 2005). To date, only one study has provided clear evidence showing that Sig-1Rs can modulate K^+ currents through a direct protein interaction in the CNS (Aydar et al., 2002).

By increasing voltage-gated K^+ currents (Kv), contingent or noncontingent cocaine exposure induces a persistent firing rate depression in the NAc shell medium spiny neurons (MSNs) (Ishikawa et al., 2009; Kourrich and Thomas, 2009; Mu et al., 2010), a brain region involved in reward-processing and motivation (Kelley, 2004). This cocaine-induced neuronal adaptation is sufficient to elicit long-lasting hyperresponsiveness to cocaine, also known as behavioral sensitization (Kourrich et al., 2012a)—a phenotype that is thought to reflect increased rewarding properties of cocaine that may contribute to the development of addictive processes (Robinson and Berridge, 2008). Interestingly, blockade of Sig-1R activity reliably attenuates cocaine-induced behavioral sensitization (Maurice and Su, 2009). However, the underlying cellular mechanisms remain unknown. Because cocaine activates the Sig-1R (Hayashi and Su, 2001), we hypothesize that the Sig-1R is a key link between cocaine exposure and the persistent decrease in NAc shell MSN intrinsic excitability that promotes behavioral sensitization to cocaine.

Here, we identify the Sig-1R as a critical molecular link between cocaine exposure and long-lasting behavioral hypersensitivity to cocaine. Knockdown of Sig-1Rs in the NAc medial shell prevented cocaine-induced persistent MSN firing rate depression and attenuated psychomotor responsiveness to cocaine. This cocaine-induced neuroadaptation occurred through Sig-1R-dependent upregulation of a subtype of

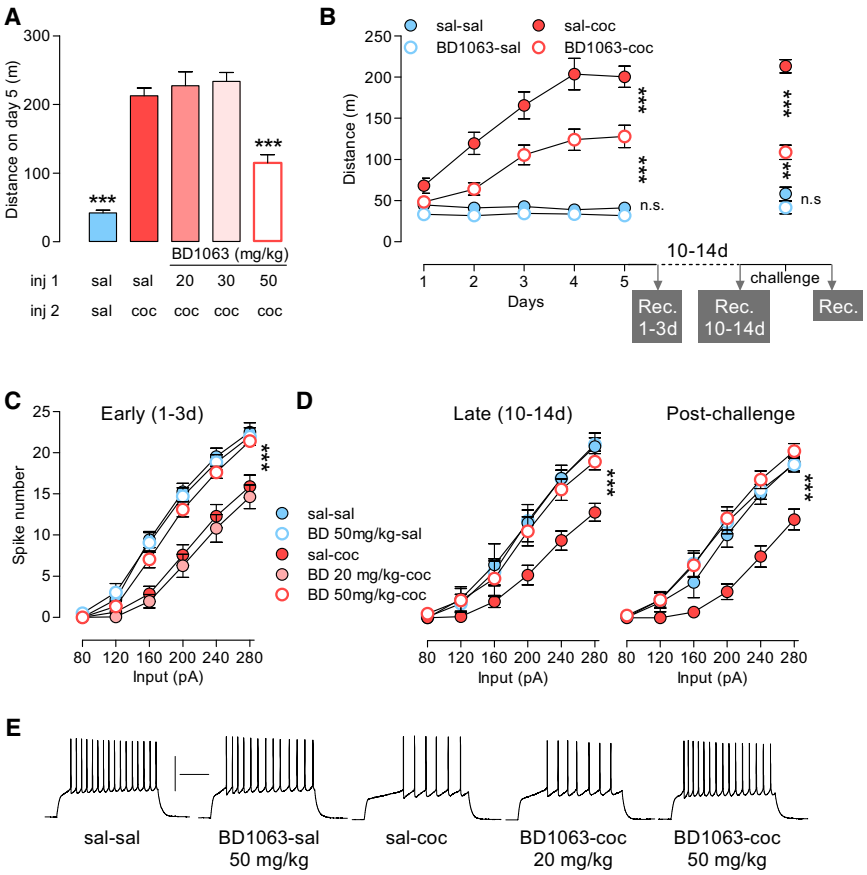

Figure 1. Effects of the Sig1R Pharmacological Blockade on Psychomotor Responsiveness to Cocaine and Accumbal Firing Are Persistent

(A) Dose-response to i.p. BD1063 (BD), a selective Sig-1R antagonist, on cocaine-induced locomotion. Injections of BD1063 or saline (inj 1) were performed 15 min prior to daily i.p. injections of cocaine (15 mg/kg) or saline (inj 2). One-way ANOVA: ***$p < 0.0001$ different from all groups.

(B–D) Cocaine-induced sensitization of locomotor activity is attenuated by inhibition of the Sig-1R with BD1063 (50 mg/kg) (n = 19–20). Ten to 14 days after the last injection a subset of animals received a cocaine (10 mg/kg) challenge injection (n = 4–9). Data indicate distance traveled during 30 min following i.p. injection of either saline or cocaine. The x-axis also represents the timeline for current-clamp recordings (Rec.). BD1063 at 50 mg/kg, but not at 20 mg/kg, prevents cocaine-induced firing rate depression when recorded at an early withdrawal time point (C) 1–3 days post-treatment, following 10–14 days of abstinence (D, left), and 24 hr after cocaine challenge injection (D, right). (C) n = 14–20 cells per group; 3–5 mice per group; in (D, left): n = 7–14 cells per group; 3–5 mice per group. (D, right) n = 8–15 cells per group; 3–4 mice per group.

(E) Sample traces at 200 pA from all groups shown in (D). Calibration: 200 ms, 50 mV. In (B), (C), and (D), two-way ANOVA: $p < 0.0001$; post hoc tests: ***$p < 0.0001$; **$p < 0.01$; n.s.: nonsignificant. Data are represented as mean ± SEM.

See also Figure S1.

transient K^+ current, the slowly-inactivating D-type K^+ current (I_D, also called I_{As}). To this end, Sig-1Rs form complexes with Kv1.2 channels at the plasma membrane. Importantly, we show that such protein-protein associations can undergo enduring experience-dependent plasticity, evidenced here by a cocaine-induced long-lasting increase in protein-protein association between Sig-1Rs and Kv1.2 channels in the NAc shell.

RESULTS

Systemic Blockade of Sig-1Rs Attenuates Behavioral Sensitivity to Cocaine through Modulation of Accumbal Firing

Sig-1R antagonists, agents that prevent Sig-1R translocation, attenuate psychomotor and rewarding effects of cocaine (Maurice and Su, 2009). To investigate the neuroanatomical site of action of Sig-1R antagonists and their functional consequences, we first used a pharmacological approach by systemically administering BD1063, a selective and prototypical Sig-1R antagonist, or BD1047, a Sig-1R antagonist that has less selectivity, however, a 10-fold higher affinity (K_i) (see Experimental Procedures for details) (Matsumoto et al., 1995). After five consecutive once-daily intraperitoneal (i.p.) injections of saline ± BD1063 (or BD1047) or cocaine ± BD1063 (or BD1047) (Figures 1A and 1B; Figure S1A available online), we assessed firing capability of MSNs with current-clamp recordings. Both Sig-1R antagonists abolished cocaine-induced firing rate depression (Figures 1C and S1B); with BD1063 at 50 mg/kg (Figures 1A and 1B) and BD1047 at 5 mg/kg (Figure S1A), doses that also attenuated psychomotor sensitization. Cocaine-induced firing rate depression in NAc MSNs, however, was preserved at lower doses of BD1063 (Figure 1C; 20 and 30 mg/kg), where animals showed normal cocaine-induced psychomotor sensitization. Further analyses showed that repeated treatment with BD1063 or BD1047 alone did not alter either basal locomotion (Figures 1B and S1A) or basal firing rate (Figures 1C and S1B). In summary, these data strongly indicate a Sig-1R-dependent mechanism as both antagonists attained similar physiological and behavioral effects despite their different pharmacological properties at the Sig-1R. Because BD1063 exhibits a higher selectivity, we used this compound in all subsequent experiments.

One hallmark of drug addiction is its persistence despite long periods of drug abstinence, as is cocaine-induced firing rate depression, an adaptation that is induced by both contingent (Mu et al., 2010) and noncontingent administration of cocaine (Ishikawa et al., 2009; Kourrich and Thomas, 2009). Consistent with previous reports, after a 2-week period of abstinence from five once-daily cocaine injections, the firing rate depression was still present; and its rescue by prior treatment with BD1063 was long-lasting as well (Figure 1D, left). Because a single re-exposure to cocaine can trigger relapse in humans and animals (Stewart, 2004), we examined the long-lasting effect

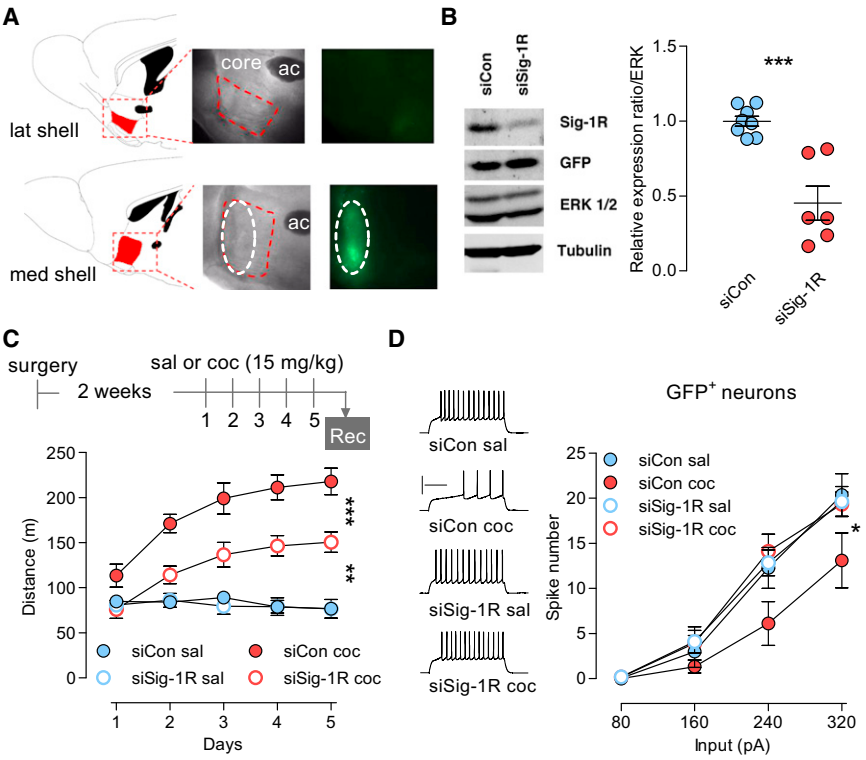

Figure 2. Knockdown of Sig-1R Protein Expression in the NAc Shell Attenuates Psychomotor Responsiveness to Cocaine and Prevents Cocaine-Induced Firing Rate Depression

(A) Sagittal brain sections showing expression of siRNA specifically in the rostro-medial shell (ML: 0.48 mm) and not lateral shell or core (ML: 0.84 mm). Diagrams and coordinates are from Paxinos and Franklin (2001).

(B) Total protein was collected after transduction and analyzed by western blotting. Left: Immunoblot showing decreased Sig-1R proteins expression. Note that GFP expression stays unchanged. Right: ERK-normalized Sig-1R protein expression shows a 50% depletion. However, this percentage is only a representative estimate of actual depletion as variability due to several factors can affect this number, including the volume of NAc shell that has been infused, protein degradation and microdissection-mediated dilution. Each data point represents NAc shell from one animal (n = 7–8). Hash marks indicate group means. Two-tailed Student's t test: ***$p < 0.001$.

(C) Top: Experimental timeline (rec, recordings). Bottom: siSig-1R attenuates psychomotor activation to chronic cocaine (n = 8–16). Data indicate distance traveled during 30 min following i.p. injection of either saline or cocaine. Two-way ANOVA: ***$p < 0.0001$. Post hoc tests: **$p < 0.01$, ***$p < 0.0001$.

(D) Left: Sample traces at 240 pA. Right: Mean number of spikes for a given magnitude of current injection was decreased in neurons from cocaine-treated animals infused with siCon, but prevented in neurons from animals infused with siSig-1R. Two-way ANOVA: *$p < 0.05$. Post hoc tests: siSig-1R coc GFP^+ is different from siCon coc and not different from any saline-treated groups. Calibration: 200 ms, 50 mV. n = 6–15 cells per group; 4–7 mice per group. Data are represented as mean ± SEM.

See also Figure S2.

of prior treatment with BD1063 on psychomotor responsiveness to cocaine re-exposure. Specifically, if BD1063 during cocaine treatment prevents sensitization mechanisms, the attenuated psychomotor sensitization should persist as well. Indeed, mice pretreated with BD1063 (BD1063-coc) still exhibited decreased psychomotor activation to a cocaine challenge (Chal) (Figure 1B). Furthermore, and as expected by our previous findings (Kourrich and Thomas, 2009), MSN firing rate was not decreased 24 hr after a single cocaine injection (Figure 1D, right). These data suggest that effects of Sig-1R blockade during cocaine treatment are long-lasting, both in terms of behavioral effects and intrinsic excitability. A possible explanation for such lasting effects may lie in blockade of functional outcomes that are triggered by cocaine-induced Sig-1R activation, in particular during abstinence or following re-exposure to a single cocaine administration. Altogether, our results indicate that the Sig-1R plays a central role in modulating the responsiveness to cocaine through modulation of accumbal firing capability.

Specific Blockade of Sig-1Rs in the NAc Shell Prevents Cocaine-Induced Behavioral and Neuronal Adaptations

To increase both regional and molecular specificity, we then employed an adeno-associated viral (AAV) vector to knockdown Sig-1R protein expression in the NAc rostro-medial shell (Figures 2A and S2A). This is the only shell region exclusively associated with purely appetitive behaviors (Reynolds and Berridge, 2002), and is most responsive to psychostimulant drugs (Ikemoto, 2010).

Knockdown of Sig-1R protein expression in the rostro-medial shell by ~50% (Figures 2B, S2B, and S2C) attenuated psychomotor activation to cocaine by ~35% (Figure 2C). When firing capability was assessed in transduced neurons (GFP^+ cells, Figure 2D), expression of Sig-1R siRNA normalized cocaine-induced firing rate depression (siSig-1R coc) to control levels (siCon sal). Additionally, AAV transduction itself (siCon or siSig-1R) did not affect basal firing levels when compared to nontransduced control cells (GFP^- neurons, Figure S2D).

Taken together, these results demonstrate that inhibition of the Sig-1R, either via systemic pharmacological antagonism or Sig-1R knockdown in the NAc rostro-medial shell attenuates psychomotor responsiveness to cocaine and counteracts cocaine-induced firing rate depression.

Cocaine-Induced NAc Shell MSN Hypoactivity Is Triggered through Sig-1R-Dependent Upregulation of a Slowly Inactivating D-type K^+ Current

Recent studies showed that repeated cocaine administration decreases NAc MSN intrinsic excitability via an increase of K^+

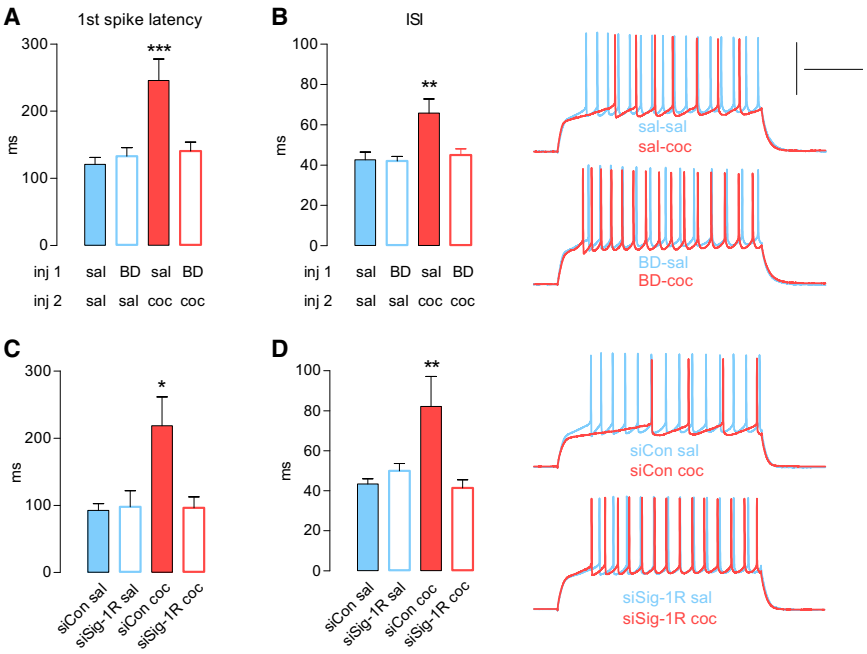

Figure 3. Cocaine-Induced Alterations in Firing Pattern Are Prevented by Both Pharmacological Blockade and Gene Knockdown of the Sig-1R

(A) Cocaine-induced increase in the latency to the fist spike is rescued by BD1063 (BD-coc). One-way ANOVA: $p < 0.0001$.

(B) Left: Cocaine-induced increase in the interspike interval (ISI) is rescued by BD1063 (BD-coc). $p < 0.005$. Right: Sample traces at 200 pA. For (A) and (B), n = 13–17 cells per group; 4–5 mice per group.

(C) Cocaine-induced increase in the latency to the fist spike (siCon-coc) is rescued by Sig-1R siRNA (siSig-1R coc) (**$p < 0.01$).

(D) Left: Cocaine-induced increase in the interspike interval (siCon-coc) is rescued by Sig-1R siRNA (siSig-1R coc) (**$p < 0.01$). Right: Sample traces at 240 pA. Calibration: 200 ms, 50 mV. For (C) and (D), n = 6–17 cells per group; 4–6 mice per group. For all panels, post hoc tests show that sal-coc and siCon coc are different from all other groups: ***$p < 0.0001$, **$p < 0.01$, *$p < 0.05$. Data are represented as mean ± SEM.

See also Figure S3.

conductances (Ishikawa et al., 2009; Kourrich and Thomas, 2009). A first step to identify these associated key K^+ currents is to quantify the observed differences in spiking patterns. We analyzed fundamental characteristics of spike trains elicited at a nonsaturating current injection that reliably elicits spikes. Spike train analysis revealed that MSNs from mice injected with cocaine showed a longer delay for spike onset (~100%, Figure 3A) and a longer interspike interval (~57%, ISI) (Figure 3B) when compared to saline-injected animals. Importantly, inhibition of Sig-1Rs with either BD1063, BD1047, or Sig-1R siRNA rescued both spike onset (Figures 3A, 3C, and S3C) and ISI (Figures 3B, 3D, and S3D).

Analysis of the action potential (AP) waveforms revealed a larger medium after-hyperpolarization (*m*AHP) (Figures S3A and S3E), a factor that determines the duration of the ISI interval and therefore results in decreased train frequency in neurons from cocaine-treated animals (Figure S3B). Medium AHP was also rescued by both BD1063 (Figure S3A) and BD1047 (Figure S3E). Consistent with a role of the Sig-1R in decreasing Na^+ current (Johannessen et al., 2009), the time taken for the spike to rise was longer (sal-sal: 0.30 ± 0.02; sal-coc: 0.36 ± 0.02 ms; $p < 0.05$). However, slowing down the AP rise did not translate into increased AP width (sal-sal: 1.29 ± 0.06; sal-coc: 1.29 ± 0.03 ms), perhaps because cocaine also increases repolarizing K^+ currents (Hu et al., 2004). Alteration in AP rise is then unlikely to play a significant role in cocaine-induced NAc MSN firing rate depression. No significant differences were observed in AP amplitude, threshold and fast AHP (data not shown).

In summary, changes in these electrophysiological components of the spike train indicate that multiple K^+ conductances are altered. In MSNs, slowly inactivating D-type K^+ currents (I_D, also called I_{As}, mediated by Kv1 family) control subthreshold excitability (delaying AP onset) and regulate repetitive discharge (Nisenbaum et al., 1994). However, because *m*AHP is also altered, SK currents may play a role (Stocker, 2004). Thus, we hypothesized that MSN firing rate depression induced by repeated cocaine is due to increased I_D and SK currents. Because I_D activates at subthreshold potentials and inactivates slowly, increased I_D would delay spike onset and increase ISI. Because SK activates after a spike, increased SK would delay occurrence of subsequent spikes, which results in increased ISI (or decreased frequency).

Thus, we investigated the potential involvement of I_D and SK currents by using toxins that selectively block these K^+ currents. We hypothesized that if repeated cocaine administration increases I_D and SK currents, toxins that block these currents should have larger effects on cells from cocaine-treated animals compared to cells from saline- or BD1063-treated animals (BD1063-sal or BD1063-coc). Following the same experimental design as described in Figure 1B (ex vivo current-clamp recordings at 10–14 days after the last injection), we found that dendrotoxin-I (DTX-I, 30 nM), a selective Kv1.x-mediated I_D blocker (Nisenbaum et al., 1994), decreased the latency to the first spike in cocaine-treated animals only (sal-coc versus sal-sal [Figures 4A and 4C]). Consistent with its role in regulating APs discharge, blocking I_D with DTX-I increased firing frequency only in the cocaine-treated group (sal-coc versus sal-sal [Figures 4B and 4C]). Effects of DTX-I on AP discharge could also be influenced by the role of I_D in AHP (Shen et al., 2004), and consequently in ISI. Indeed, I_D inhibition with DTX-I restored both the ISI (sal-sal: 44.34 ± 2.05; sal-coc: 85.74 ± 9.83; sal-coc + DTX-I: 50.76 ± 6.32 ms; one-way ANOVA, $p < 0.01$) and *m*AHP levels (sal-sal: 8.48 ± 1.34; sal-coc: 10.85 ± 0.34; sal-coc + DTX-I: 7.84 ± 0.70 ms; one-way ANOVA, $p < 0.0001$) to control levels (sal-sal). Furthermore, specific DTX-induced modulations of firing patterns translated to increased NAc shell MSN AP firing selectively in

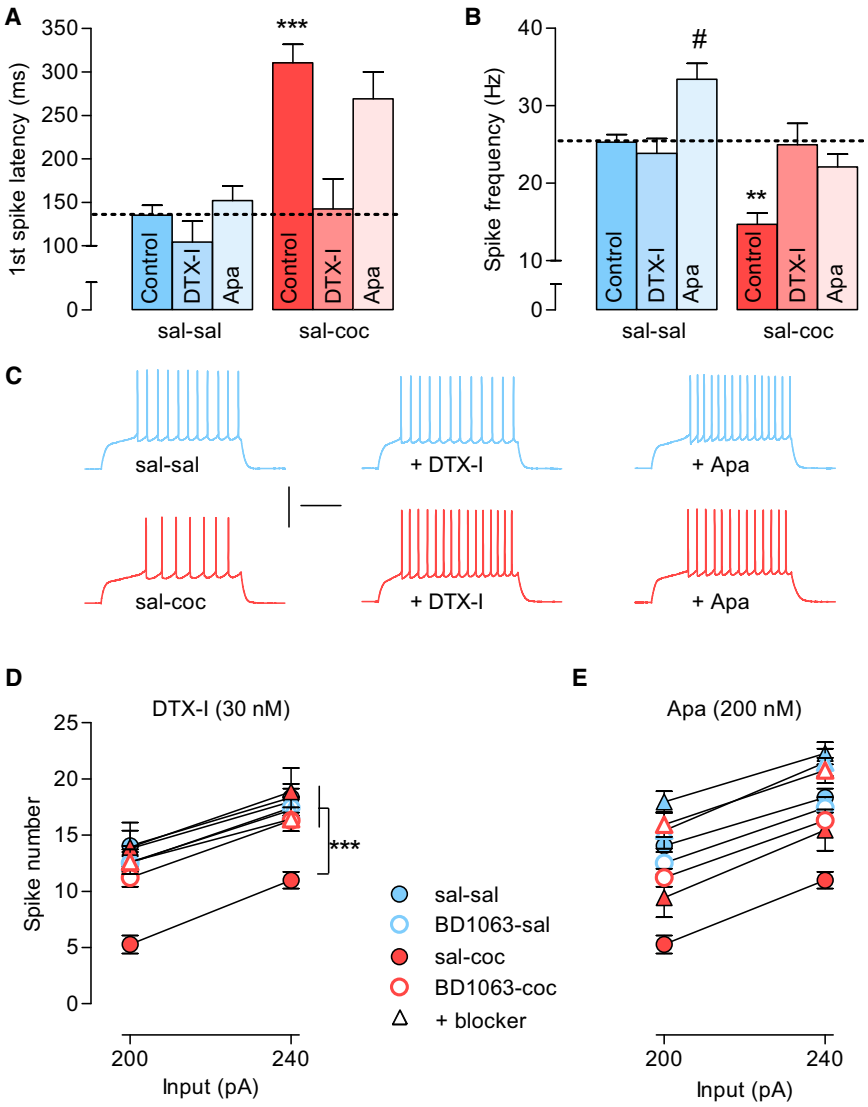

Figure 4. Cocaine-Induced Shell MSN Hypoactivity Is Triggered through Sig-1R-Dependent Upregulation of the D-Type K^+ Current

(A) I_D inhibition with DTX-I (30 nM) but not SK inhibition with Apa (200 nM) rescues cocaine-induce increase in the latency to the first spike. One-way ANOVA: $p < 0.0001$; post hoc analysis: ***$p < 0.0001$, sal-coc group is different from all other groups except sal-coc + Apa. Dashed lines represent basal level for sal-sal control group.

(B) Although I_D inhibition with DTX-I (30 nM) specifically rescues cocaine-induce decrease in the spike frequency, SK inhibition with Apa (200 nM) increases spike frequency in both control (sal-sal) and cocaine-treated group (sal-coc). One-way ANOVA: $p < 0.0001$. Post hoc analysis: **$p < 0.001$, sal-coc group is different from all other groups; #$p < 0.05$, sal-sal is different from sal-sal + Apa. Dashed lines represent basal level for sal-sal control group. In (A) and (B), values correspond to parameters measured at 200 pA current injection.

(C) Sample traces at 200 pA from sal-sal and sal-coc groups before and after toxins.

(D) In cells from cocaine-treated animals, DTX-I renormalizes the number of spikes to control levels without affecting any other groups. For clarity, only number of spikes at 200 and 240 pA are presented, however, statistical analysis was performed on the entire range of current injections (from 80 to 280 pA with 40 pA increment; two-way ANOVA, $p < 0.0001$). Post hoc analysis: sal-coc group is significantly different from any other groups.

(E) Apamin positively shifts number of spikes in all groups. Two-way ANOVA: $p < 0.0001$; post hoc analysis: all groups + blocker are significantly different from their respective group with no blocker. Calibration: 200 ms, 50 mV. For all panels, n = 5–28 cells per group; 3–11 mice per group. Data are represented as mean ± SEM.

See also Figure S4.

cocaine-treated animals (sal-coc) without altering firing level in any other group (sal-sal, BD1063-sal and BD1063-coc) (Figure S4), an effect that normalized MSN firing rate depression to control levels (sal-sal) (Figure 4D). These results suggest that chronic cocaine administration depresses MSN firing rate through upregulation of I_D.

Cocaine-induced increase in *m*AHP, a component that is influenced by SK current, may also contribute to the decreased firing frequency. Although the effects are opposite, two recent studies suggested that both cocaine (Ishikawa et al., 2009) and the Sig-1R (Martina et al., 2007) can modulate SK currents. Thus, we investigated a potential role for SK in cocaine-induced firing adaptation using the selective blocker apamin. SK inhibition with apamin (Apa) decreased *m*AHP to the same extent independent of cocaine treatment (e.g., delta from respective control at 200 pA: sal-sal + Apa = 1.6 ± 0.73; sal-coc + Apa = 2.3 ± 0.38 mV; $p > 0.05$), which translated into increased frequency in both groups (sal-sal and sal-coc [Figures 4B and 4C]). As expected, because SK is not activated at subthreshold potential, apamin did not alter the latency to the first spike (Figure 4A). Furthermore, apamin-induced modulation of *m*AHP led to a similar increase in NAc shell MSN AP firing in all behavioral groups (Figures 4E and S4). Analysis of a wide range of depolarizing current injections eliciting either low or high spike frequency (from 160 to 280 pA) did not reveal differential effects of apamin in any of the experimental groups, which indicates that 200 nM apamin is not a saturating and thereby potentially confounding dose. Our results suggest that SK current is unlikely to play a role in cocaine-induced MSN hypoactivity.

Finally and because pretreatment with BD1063 (BD1063-coc group) occluded subsequent effects of DTX-I but not apamin (Figures 4D, 4E, and S4), our results indicate that long-lasting psychomotor responsiveness to cocaine is maintained via Sig-1R-dependent upregulation of the transient slowly-inactivating K^+ current I_D.

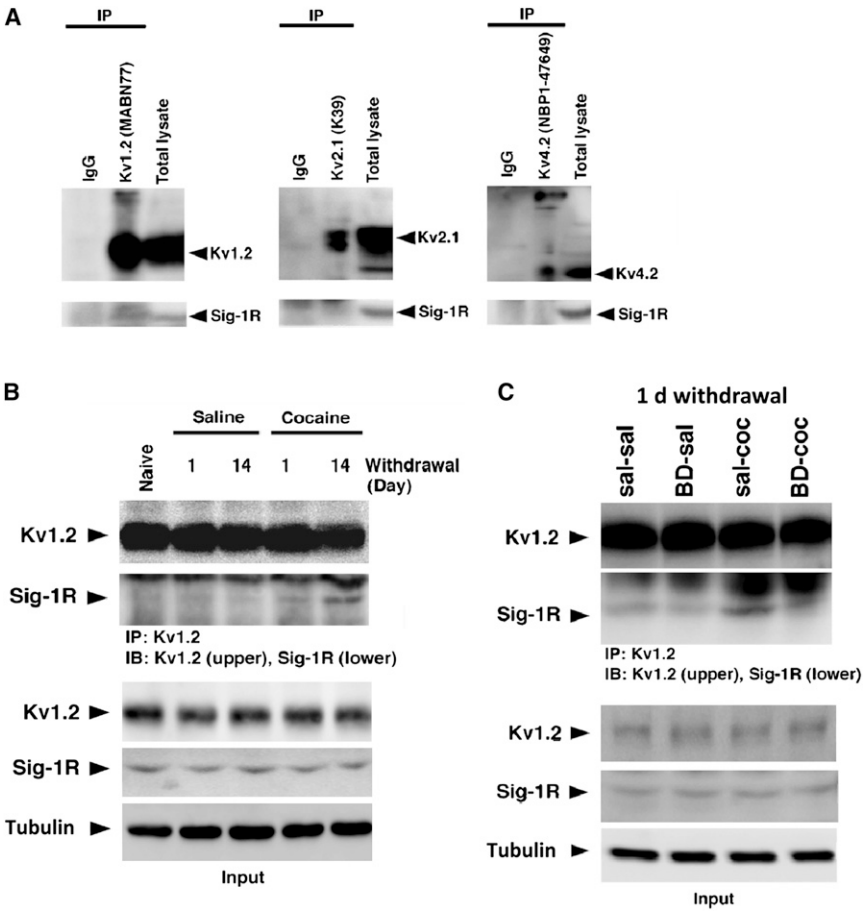

Figure 5. Repeated In Vivo Cocaine Upregulates Physical Association of Sig-1Rs with Kv1.2 α-Subunits

(A) Postnuclear cell lysates were prepared from NAc medial shell tissue, immunoprecipitated with anti-Kv1.2, -Kv2.1, and -Kv4.2 antibodies or with normal immunoglobulins as control (IgG), then probed with anti-Sig-1R antibody. Only Kv1.2 coimmunoprecipitated Sig-1R (left panel, middle lane). Arrowheads indicate the position of the monomeric form of respective proteins. Kv1.2 and 4.2 also show oligomeric forms at the top of the images.

(B) Cell lysates from NAc medial shell tissue were prepared from drug-naive, saline, and cocaine-treated groups collected at both early (1 day) and late abstinence time points (14 days). Samples were immunoprecipitated with the anti-Kv1.2 antibody and probed with the anti-Kv1.2 (upper) or the anti-Sig-1R antibody (lower). Top: Repeated cocaine enhances Sig-1Rs coimmunoprecipitation with Kv1.2 (lane 4), an effect that is further increased after 14 days of protracted abstinence (lane 5). Bottom: Immunoblots quantifying total protein levels of Sig-1Rs and Kv1.2 subunits. Note that the protein levels remained unchanged throughout cocaine abstinence.

(C) In a different set of animals, cell lysates of NAc medial shell tissue were prepared from saline ± BD1063 (sal-sal and BD-sal) and cocaine ± BD1063 (sal-coc and BD-coc) following the same experimental design as in Figure 1. Tissue was collected on the day following the last injection. Top: BD1063 prevents Sig-1Rs to coimmunoprecipitate with Kv1.2 (lane 4). Bottom: Immunoblots quantifying total protein levels of Sig-1Rs and Kv1.2 subunits. Note that protein levels remained unchanged following either of the treatment. Assays were performed with two samples per group, where each sample was prepared by combining NAc medial shell tissue pooled from 4–5 mice.

See also Figure S5.

The Sig-1R Upregulates I_D through Physical Association with Kv1.2 Channel

Increasing evidence from in vitro studies suggests that Sig-1R-dependent modulation of K^+ currents may occur through direct protein-protein interaction to either modulate K^+ channel function (Aydar et al., 2002; Kinoshita et al., 2012) or to regulate subunit trafficking (Crottès et al., 2011). We thus tested the hypothesis that activation of Sig-1Rs increases I_D currents through physical interaction with K^+ channel α-subunits that are known to generate I_D in MSNs. Although many Kv1.x channel subunits that are expressed in MSNs can contribute to the generation of I_D, including Kv1.1, Kv1.2, and Kv1.6 (*Shaker* family), Shen et al. (2004) demonstrated that Kv1.2 channels, but not Kv1.1 or Kv1.6, control the latency to the first spike and repetitive AP discharge. In addition, Kv2.1 channels (*Shab* family, mediating *I*K current), which colocalize with Sig-1Rs (Mavlyutov et al., 2010), and Kv4.2 channels (*Shal* family, mediating the fast-inactivating A-type K^+ currents I_{Af}), are both highly expressed in striatal neurons (Vacher et al., 2008), and also regulate subthreshold voltage behavior, firing frequency, and voltage trajectory after spikes. To determine whether Kv1.2, Kv2.1, and/or Kv4.2 physically interact with Sig-1Rs, we performed coimmunoprecipitation experiments using membrane lysates from the NAc medial shell. We found that a marginal, yet detectable level of Sig-1Rs was coimmunoprecipitated with Kv1.2 (Figure 5A), and that no visible interaction between Kv2.1 or Kv4.2 and Sig-1Rs was detected, suggesting that in a basal state a fraction of Sig-1Rs form a complex with Kv1.2 channels in the NAc shell. We also observed similar results in mouse prefrontal cortex (Figure S5A), suggesting that the association between Kv1.2 and Sig-1Rs may not be restricted to the NAc but may also occur elsewhere in the brain.

Because cocaine experience leads to an enduring Sig-1R-dependent upregulation of a DTX-sensitive K^+ current, we then tested if cocaine upregulates interactions between Sig-1Rs and Kv1.2 channels in the NAc medial shell. Compared to controls, cell lysates from cocaine-treated mice exhibit higher binding levels between Sig-1Rs and Kv1.2 channels after one day of abstinence (Figures 5B and S5B), an effect that is prevented by BD1063 (Figures 5C and S5C, left). Interestingly, this physical interaction seems to be further increased following a protracted abstinence period of 14 days (Figures 5B and S5B). Immunoblot quantification of cell lysates indicates that total protein levels of Sig-1Rs and Kv1.2 subunits were not

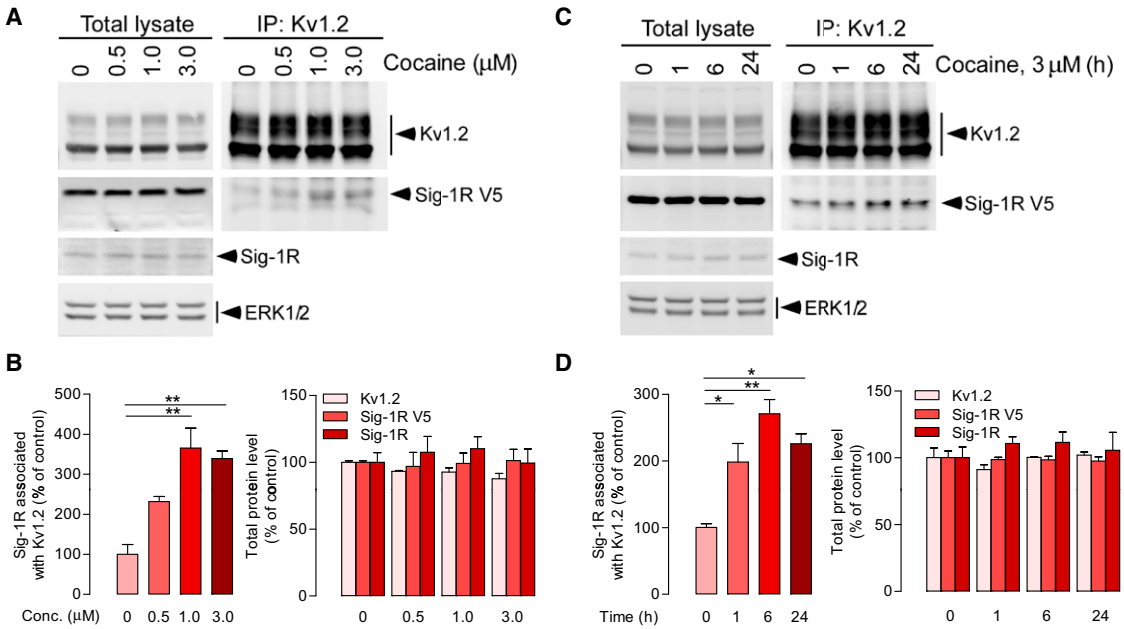

Figure 6. Cocaine Enhances the Interaction between Sig-1R and Kv1.2 α-Subunit in NG108-15 Cells

(A–D) NG 108-15 cells were transfected with pcDNA3.1-Sig-1R-V5-His and pCMV6-Kv1.2 plasmids to overexpress Sig-1R-V5 and Kv1.2, respectively. Sig-1R-V5- and Kv1.2-overexpressing NG108-15 cells were treated with different doses of cocaine as indicated for 6 hr (A and B) or with 3 μM of cocaine for different periods of time (0, 1, 6, and 24 hr) (C and D). Cell extracts were then immunoprecipitated with the anti-Kv1.2 antibody followed by immunoblotting using anti-Kv1.2 or anti-V5 antibody, respectively. The protein level of endogenous Sig-1Rs was detected using anti-Sig-1R antibody, and ERK1/2 was used as the loading control. Cocaine increases Sig-1R and Kv1.2 binding (A and B, left, one-way ANOVA: treatment, $p < 0.001$) (C and D, left, one-way ANOVA: treatment, $p < 0.01$). In (B) and (D) (left panels), post hoc tests when compared to control (0 μM or 0 hr), $^*p < 0.05$, $^{**}p < 0.01$. Consistent with NAc ex vivo studies (Figure 5), cocaine did not change protein levels of Sig-1Rs and Kv1.2 α-subunits (B and D, right). The graph represents means ± SEM from three independent experiments.
See also Figure S6.

different among groups, and remained unchanged across all time points (Figures 5B and S5C, right). Taken together, our data suggest that Sig-1Rs form protein complexes with Kv1.2 channels in the NAc medial shell; and that this complex formation is increased upon cocaine experience.

These results are of particular importance as they provide evidence that the specific protein-protein interaction involving Sig-1Rs and Kv channels represent an element constituting experience-dependent neuronal plasticity in the NAc caused by cocaine exposure.

Cocaine Induces Trafficking of Sig-1Rs and Kv1.2 to the Plasma Membrane

Upon cocaine exposure, Sig-1Rs form additional physical associations with Kv1.2 channels to upregulate I_D current. Because total protein levels of Sig-1Rs and Kv1.2 α-subunits were not different between saline- and cocaine-treated animals (Figures 5B and 5C), it appears likely that increased Sig-1R and Kv1.2 association may not be driven by transcriptional modifications of Sig-1R or Kv1.2 proteins per se, but rather by translocation of Sig-1Rs from the ER to the plasmalemma and binding to a pre-existing pool of Kv1.2 channels. However, because Sig-1Rs can also modulate K^+ currents through the regulation of subunit trafficking activity (Crottès et al., 2011), it is possible that Sig-1Rs also traffic mature Kv1.2 channels from the ER to the plasmalemma.

To differentiate between these two scenarios, we overexpressed the Sig-1R and Kv1.2 subunits in the NG108-15 cell line. As in the NAc shell, Sig-1Rs bound to Kv1.2 channels in a basal state (Figure S6Aa and S6Ab, fourth lane) and cocaine bath application (3 μM, 6 hr) increased the binding (Figure S6Ba, compare 4th and 5th lane), an effect that is also observed in the neuro-2A cell line (Figure S6Bb). Furthermore, the cocaine-induced increase in Sig-1R and Kv1.2 binding is seemingly dose- (Figures 6A and 6B left) and time-dependent (Figure 6D, left). Consistent with the NAc ex vivo study (Figures 5 and S5C), cocaine did not change protein levels of Sig-1Rs and Kv1.2 α-subunits (Figures 6B and 6D, right), suggesting a cocaine-triggered subcellular redistribution of Sig-1Rs and Kv1.2 channels. Indeed, immunofluorescence double-labeling with anti-V5 (Sig-1R, green) and anti-Kv1.2 (red) antibodies revealed that cocaine (3 μM, 6 hr) promotes colocalization of Kv1.2 and Sig-1Rs at the cellular surface (Figure 7A). Next, to provide direct evidence for the Sig-1R and Kv1.2 trafficking to the plasma membrane we used cell surface immunoprecipitation and biotinylation methods, respectively. Beforehand, we demonstrated that cocaine decreased a small portion of Sig-1Rs at the MAM (Figures S7A and S7B). As the aim of this experiment was to test for a cocaine-induced decrease of Sig-1Rs specifically at the MAM, we then performed assays using NG108-15 cells to address whether Sig-1Rs subsequently move to the plasma membrane. Because N and C termini of

the Sig-1R are lumenal (Hayashi and Su, 2007), Sig-1R termini should upon translocation to the plasma membrane face the extracellular space. Using antibodies that specifically target N and C termini of the Sig-1R we showed that Sig-1Rs were present at the plasma membrane and that cocaine (3 μM, 6 hr) further increased their levels by ~75% (Figure 7B). Our data reveal that Sig-1Rs can be fully integrated into the phospholipidic layers rather than translocating at the inner leaflet of the plasma membrane. Next, we performed a biotinylation assay to detect the Kv1.2 subunit on the surface of the plasma membrane. Cocaine (3 μM, 6 hr) increased membrane levels of Kv1.2 channels in both NG108-15 (Figure 7C) and neuro-2a cells (Figure S7C), an effect that was amplified by overexpression of the Sig-1R (+ pEYFP-Sig-1R) and prevented by Sig-1R knockdown with AAV-siSig-1R (Figure 7C). These results demonstrate that the cocaine-induced increase in membrane Kv1.2 channels is a consequence of Sig-1R activation.

To assess functional outcomes of this effect, we have combined electrophysiological and pharmacological approaches and directly measured DTX-I - sensitive currents from the total K^+ currents in NAc shell MSNs. Consistent with the specific effect of DTX-I on cocaine-induced firing rate depression, repeated cocaine administration increased DTX-I-sensitive currents (sal-coc versus sal-sal; sal-sal: ~720 pA; sal-coc: ~1,700 pA), which was prevented by pretreatment with BD1063 (BD-coc group) (Figures 7D and 7E).

DISCUSSION

Our studies demonstrate that the accumbal Sig-1R enhances long-lasting behavioral sensitivity to cocaine through a decrease of neuronal intrinsic excitability—an effect that is induced by Sig-1R-dependent upregulation of I_D. Furthermore, we provide evidence that in a basal state Sig-1Rs physically interact with Kv1.2 channels in the CNS—a channel that mediates I_D in MSNs (Shen et al., 2004). Importantly, our data suggest that long-lasting behavioral sensitivity to cocaine is in part due to a persistent upregulation of the Sig-1R and Kv1.2 complex in the NAc shell. In vitro studies in cell lines suggest that this event occurs at the plasma membrane, however, ex vivo recordings in NAc shell provided functional evidence that such phenomenon may also occur in vivo.

Target Specificity

When investigating the role of the Sig-1R, ligand specificity is a major limiting factor. Therefore, to provide strong evidence for the involvement of the Sig-1R in the phenomena investigated in the present study, we used a multi-approach strategy including pharmacological tools, gene knockdown and biochemical assays (ex vivo and in vitro). First, we pharmacologically targeted the Sig-1R with two highly selective antagonists, BD1063 and BD1047 (Matsumoto et al., 1995). We found that both BD1063 (50 mg/kg) and BD1047 (5 mg/kg) attenuated cocaine-induced psychomotor sensitization in a similar manner and prevented cocaine-induced firing rate depression in NAc neurons (Figures 1, S1, 3, and S3). Second, we used an AAV-siRNA targeting the Sig-1R protein expression. Effects of the Sig-1R siRNA yielded similar behavioral and physiological results as BD1063 and BD1047 (Figures 2 and S2). Third, repeated administration of cocaine upregulated Kv1.2-mediated I_D currents. If the Sig-1R was not a major mediator of this effect, increased cocaine-induced Sig-1R and Kv1.2 channel binding (in vivo in NAc shell and in vitro using NG108-15 and neuro-2a cell lines) and binding blockade by in vivo BD1063 would have been unlikely (Figures 5, S5, 6, S6, and S7C). And last, overexpression or knockdown of the Sig-1R in vitro enhanced or prevented the cocaine-induced increase in membrane Kv1.2 channels respectively (Figure 7C), which demonstrates a causal relationship between the cocaine-induced increase in membrane Kv1.2 channels and Sig-1R activation. Taken together, results from our multi-approach strategy all converge toward a major role for accumbal Sig-1Rs in long-lasting effects of cocaine on both behavioral response to the drug and MSN firing rate.

Plasticity of the Sig-1R and Kv1.2 Complex: A Candidate Substrate for Long-Lasting Cocaine-Induced MSN Firing Rate Depression

Our data suggest that Sig-1R and Kv1.2 channel interaction is constitutive and/or occurs with endogenous agonists. The Kv1.2-mediated current plays a major role in controlling fundamental parameters that determine neuronal communication in striatal MSNs (Shen et al., 2004). This includes the capability of neurons to transition from silent to firing mode and the regulation of the interspike interval—a major parameter that tightly controls the frequency-modulated code that is characteristic of neurons (Hille, 2001). Recently, in vitro studies showed that the Sig-1R, via physical association, modulates K^+ currents either through the regulation of subunit trafficking (Crottès et al., 2011) or via ligand-independent modulation of channel function (Kinoshita et al., 2012). Taken together, the Sig-1R is emerging as a potential auxiliary subunit for voltage-gated K^+ channels that is reminiscent of the already documented auxiliary β or KChip subunits (Vacher et al., 2008)—an idea first proposed by Jackson's group, which demonstrated in *Xenopus* oocytes that the Sig-1R, through physical association and in ligand-independent manner, regulates Kv1.4-mediated currents (Aydar et al., 2002).

Putative Sig-1R-Dependent Synergetic Pathways in Cocaine-Induced Accumbal Hypoactivity

The present findings suggest a mechanism initiated by the Sig-1R that is linked to behavioral sensitivity to drugs of abuse, however, other cocaine-triggered Sig-1R signaling pathways may also contribute to the decreased shell MSN excitability. As the primary consequence of cocaine exposure is the accumulation of extracellular dopamine (DA) following DA transporter blockade, excess DA receptor (DAR) activation has been a prominent hypothesis for cocaine-induced changes in firing rate (Hopf et al., 2003; Perez et al., 2006). However, a recent study uncovered a cocaine-mediated signaling pathway that is independent of DA transporter blockade (Navarro et al., 2010). Sig-1Rs and DA 1 receptors (D1Rs) can form heteromers and when cocaine binds to this complex it amplifies D1R-mediated increases in cyclic AMP (cAMP). Cyclic AMP-dependent PKA activation regulates the striatal slowly-inactivating A-type K^+

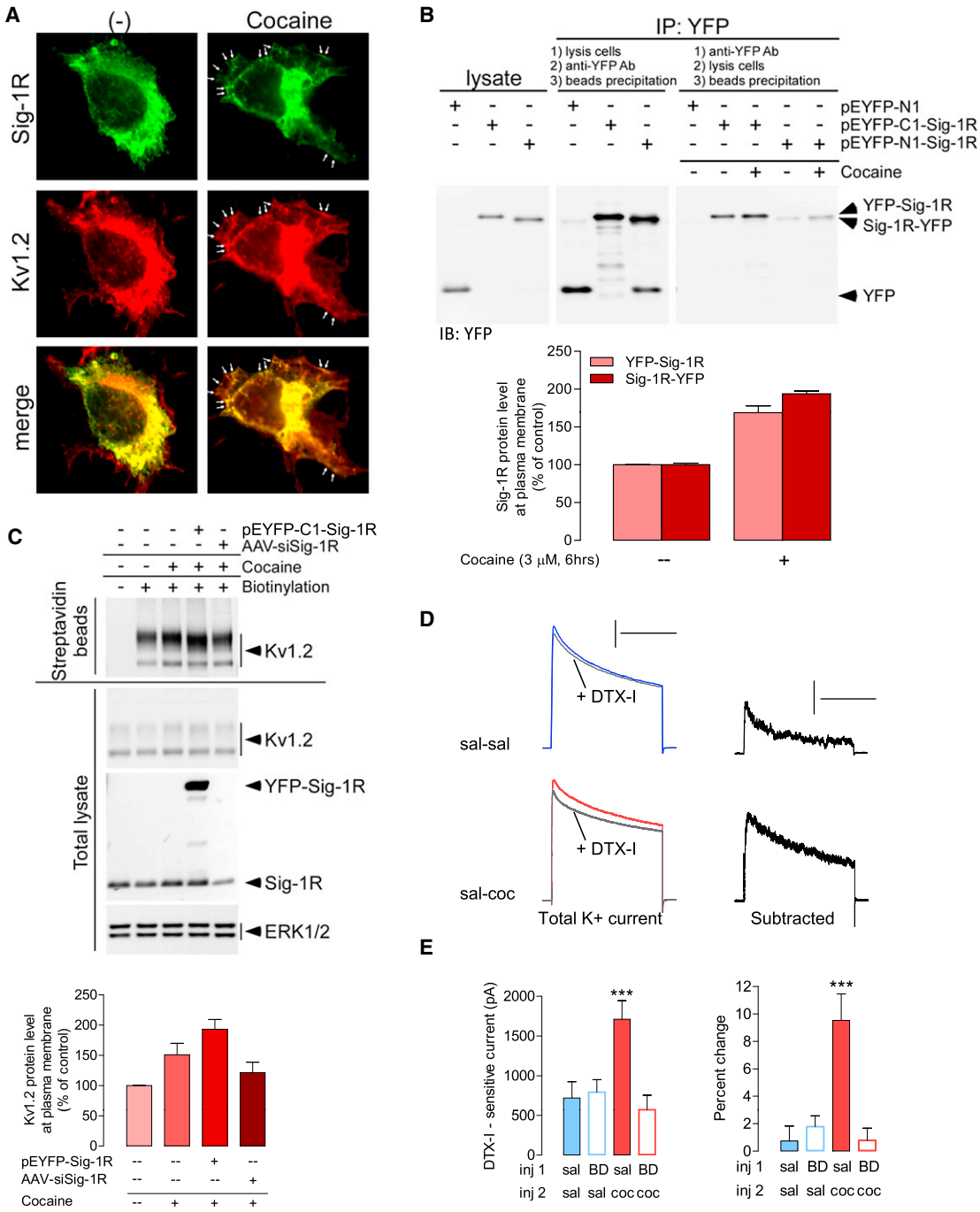

Figure 7. Cocaine Treatment Increases the Localization of Sig-1R and Kv1.2 α-Subunit at the Plasma Membrane

(A) In NG108-15 cells, cocaine (3 μM, 6 hr) increases colocalization (arrowheads indicate puncta) of Kv1.2 (red) and Sig-1R (green) at the cellular surface.

(B) NG108-15 cells were transfected with pEYFP-N1, pEYFP-C1-Sig-1R, or pEYFP-N1-Sig-1R to express YFP, YFP-Sig-1R, or Sig-1R-YFP, respectively. Cocaine (3 μM, 6 hr) increases Sig-1Rs at the membrane (blot in right) by ~80% (bottom). Variations in the procedure between immunoprecipitation assays are indicated on the figure and described in Experimental Procedures. Differences in the intensity between the immunoblotting for the YFP-Sig-1R versus Sig-1R-YFP may reflect differential receptor trafficking activity following the addition of YFP to either the N- or the C-terminal. Another explanation may lie in the different conformation of YFP-Sig-1R and Sig-1R-YFP at the surface and thereby differentially affecting the accessibility of antigenic sites of YFP to the detecting antibody. Nonetheless, cocaine enhances the surface expression of both YFP-Sig-1R and Sig-1R-YFP.

(C) Kv1.2-overexpressing NG108-15 cells were cotransfected with pEYFP-C1-Sig-1R or AAV-siSig-1R as indicated. Cocaine (3 μM, 6 hr) increases biotinylated Kv1.2 (streptavidin beads panel), but not total Kv1.2 (total lysate panel). ERK1/2 was used as the loading control. Bottom: Immunoblot quantifications showing that cocaine (3 μM, 6 hr) increases membrane levels of Kv1.2 channels, an effect that is amplified by overexpression of the Sig-1R (+ pEYFP-C1-Sig-1R) and prevented by Sig-1R knockdown with AAV-siSig-1R. The graphs represent means ± SEM from two independent experiments.

(legend continued on next page)

current I_D (Hopf et al., 2003; Perez et al., 2006). However, in those studies, inhibiting PKA pathways decreases AP firing. Therefore, one might expect that cocaine binding to D1R-Sig-1R heteromers, which amplifies PKA signaling, would result in increased firing—an effect that is opposite to what we have observed. Although the complex formed by the D1R and the Sig-1R likely plays a role in the behavioral effects of cocaine, the signaling pathway that is initiated does not seem to result in changes in intrinsic postsynaptic neuronal excitability; perhaps, based on previous studies, one role for D1R-Sig-1R complexes is to modulate presynaptic glutamate release (Dong et al., 2007).

Another possibility involves αCaMKII, a strong modulator of fast-inactivating A-type K^+ current (I_{Af}) (Varga et al., 2004)—a current that may regulate MSN firing rate (Varga et al., 2000). A recent report showed that a transgenic mouse line overexpressing a constitutively active form of striatal-specific αCaMKII exhibits decreased intrinsic excitability in the NAc shell, which enhances cocaine reward, including psychomotor sensitization and conditioned place-preference (Kourrich et al., 2012a). Although the activated form of αCaMKII (CaMKII-pThr286) seems to occur through a D1R-dependent mechanism (Anderson et al., 2008), recent data suggest that activation of the Sig-1R also has the capability to increase αCaMKII-pThr286 (Moriguchi et al., 2011). Whether this mechanism results in modulation of neuronal firing is yet to be investigated. If so, this mechanism could represent an additional synergetic pathway through which cocaine-induced Sig-1R activation indirectly modulates shell neuronal excitability.

Data-Based Model

In drug-naive animals, Sig-1Rs may constitutively regulate Kv1.2 channels to control MSN firing capability. Cocaine can bind to Sig-1Rs at a reward-relevant concentration (Chen et al., 2007; Kahoun and Ruoho, 1992), which triggers the Sig-1R to dissociate from the Binding immunoglobulin Protein (BiP), another ER chaperone protein that in absence of ligands prevents the Sig-1R from translocating to the plasmalemma (Hayashi and Su, 2003; Su et al., 2010). Repeated exposure to cocaine causes intracellular Sig-1Rs to persistently bind to Kv1.2 α-subunits and to traffic from the ER to the plasma membrane, which enhances I_D. As a result, shell MSN intrinsic excitability is decreased—an adaptation that can promote appetitive reward-seeking behaviors (Kelley, 2004; Krause et al., 2010; Taha and Fields, 2006) and that is potentially involved in encoding the positive hedonic qualities of a stimulus (Carlezon and Thomas, 2009).

In conclusion, the functional consequence of the long-lasting interaction of Sig-1Rs and Kv1.2 channels represents a mechanism that shapes cocaine-dependent neuronal excitability. Whether this mechanism is involved in the development of drug addiction is yet to be investigated. Nonetheless, drug addiction is a chronic neuropsychiatric disorder characterized by its long-lasting vulnerability to relapse. Preventing the development of such a phenomenon by targeting the Sig-1R may provide complementary means to cope with this disease. However, because the Sig-1R, via interaction with various proteins (Kourrich et al., 2012b), is involved in a plethora of signaling pathways, directly targeting the Sig-1R is likely going to interfere with other cellular mechanisms and may lead to unwanted or potentially dangerous side effects. Therefore, and as shown here for the Sig-1R and Kv1.2 binding, the next step is clearly to establish a causal relationship between specific Sig-1R-protein associations and physiological outcomes, a step that will bolster the development of efficient therapeutic tools that disrupt specific bindings. This advancement in basic cellular mechanisms will not only contribute to the development of treatment for drug addiction but also for other chronic diseases, including Alzheimer's disease, multiple sclerosis, neuropathic pain, and cardiac pathologies where both plasticity of intrinsic excitability and Sig-1Rs are engaged, some of which may occur through persistent Sig-1R binding to voltage-gated channels. Such innovation will certainly provide avenues to target specific Sig-1R-related afflictions.

EXPERIMENTAL PROCEDURES

Drug Treatment Regimen and Behavior

Male C57BL/6J mice (4–5 weeks of age) were habituated to the animal colony for 1 week before testing. For experiments in Figure 2, intra-NAc medial shell AAV-siRNA (containing either siCon, inactive siRNA; or siSig-1R, Sig-1R siRNA; Figure S2D) was infused 2 weeks before testing. In this experiment, mice were 7–8 weeks of age at the time of surgery. For all experiments, mice were group housed and maintained on a 12 hr light/dark cycle (light on at 7:00 AM). On each of the five consecutive testing days (between 10:00 AM and 2:00 PM), mice were transferred from the animal colony to a testing room and placed individually into activity arenas (clear rectangular box, 13 × 15.5 × 7.5 inches). See Extended Experimental Procedures for details. The experimental procedures followed the Guide for the Care and Use of Laboratory Animals (eighth edition) and were approved by the Animal Care and Use Committee.

Drugs

1-[2-(3,4-Dichlorophenyl)ethyl]-4-methylpiperazine (BD1063, Tocris) and N-[2-(3,4-dichlorophenyl)ethyl]-N-methyl-2-(dimethylamino)ethylamine (BD1047, Tocris) have preferential affinities for Sig-1R sites, with K_i values of ~9 nM and ~0.9 nM, respectively. BD1063 has a 49-fold greater affinity for Sig-1R sites than Sig-2R sites. BD1047, likewise, has a 51-fold greater affinity for Sig-1R binding sites compared to Sig-2R sites (Matsumoto et al., 1995). BD1063 and cocaine hydrochloride were dissolved in 0.9% NaCl, and BD1047 in distilled water. Drugs were injected i.p. at a volume of 10 ml/kg.

(D) Left: K^+ current traces in control solution and during bath application of DTX-I (30 nM) in sal-sal and sal-coc groups. Currents were evoked by depolarizing test pulses to + 30 mV after a prepulse of 2 s to −90 mV. Calibration: 500 ms, 5 nA. Right: Subtraction of current trace obtained in the presence of DTX-I from control solution. Calibration: 500 ms, 1 nA.

(E) Repeated cocaine administration following the same experimental design as in Figure 1 (recordings at 10–14 days of abstinence) increases DTX-I-sensitive K^+ current (left), a change that corresponds to an ~10% blockade in cocaine-treated animals compared to ~1% in control group [(pre-DTX − post-DTX)/pre-DTX × 100]. ANOVA: ***$p < 0.0001$. Post hoc analysis for left and right panels: sal-coc is different from all other groups. n = 7–10 cells per group; 4 mice per group. The graphs represent means ± SEM.

See also Figure S7.

Slice Preparation and Solutions

Sagittal slices of the NAc shell (240 μm) were prepared as described previously (Kourrich and Thomas, 2009). Slices recovered in a holding chamber for at least 1 hr before use. During recording they were superfused with artificial cerebro-spinal fluid (ACSF) (31.5°C–32.5°C) saturated with 95% O_2/5% CO_2 and containing (in mM) 119 NaCl, 2.5 KCl, 1.0 NaH_2PO_4, 1.3 $MgSO_4$, 2.5 $CaCl_2$, 26.2 $NaHCO_3$, and 11 glucose. During recordings, ACSF containing picrotoxin (100 μM) was used to block $GABA_A$ receptor-mediated inhibitory postsynaptic potentials and kynurenic acid (2 mM) to block glutamate receptors. For voltage-clamp experiments investigating I_D (DTX-I-sensitive current) (Figures 7D and 7E), voltage-dependent Na^+, Ca^{2+}, and Ca^{2+}-dependent K^+ currents were blocked with TTX (500 nM) and $CdCl_2$ (100 μM). See Extended Experimental Procedures for details.

Electrophysiology

To quantify firing properties, whole-cell current-clamp recordings were performed with electrodes (3–5 MΩ) containing 120 K-gluconate, 20 KCl, 10 HEPES, 0.2 EGTA, 2 $MgCl_2$, 4 Na_2ATP, and 0.3 Tris-GTP at a pH of 7.20–7.25. Data were filtered at 5 KHz, digitized at 10 kHz, and collected and analyzed using Clampex 10.3 software (Clampex 10.3.0.2, Molecular Devices). Membrane potentials were maintained at –80 mV, series resistances (10–18 MΩ) and input resistances were monitored on-line with a 40 pA current injection (150 ms) given before each 700 ms current injection stimulus. Only cells with a stable *Ri* (Δ < 10%) for the duration of the recording were kept for analysis. The value of each parameter for a given cell was the average value measured from 2 to 4 cycles (experiments in Figure 1: 700 ms duration at 0.1 Hz, –80 to +280 pA range with a 40 pA step increment; experiments in Figure 2: 700 ms duration at 0.1 Hz, 0 to +320 pA range with a 80 pA step increment). For experiments in Figure 2, recordings from the two time points (1–3 days and 10–14 days) yielded similar effects per groups, therefore data from each group were pooled. See Extended Experimental Procedures for details on the method for quantifying differences in firing pattern and APs waveform.

K^+ channel blockers (dendrotoxin-I, DTX-I at 30 nM; or apamin, Apa at 200 nM; Sigma-Aldrich) were either bath applied during recordings or administered in holding chambers containing brain slices. Because these two methods yielded similar effects per groups, data from each group were pooled.

For experiments in Figures 7D and 7E, voltage-clamp protocols to measure D-type K^+ currents consisted of a voltage-step command from a holding potential of −80 mV. The neuron was hyperpolarized to −90 mV for 2 s and then to +30 mV for 1 s. Algebraic isolation of I_D was performed by subtracting the current evoked in the presence of the I_D channel blocker DTX-I (30 nM) from currents evoked in control solution. The peak current amplitude for each voltage command was calculated from the average of three to five traces. Leak subtraction was not performed, and series resistance was compensated at 60%.

AAV siRNA Vectors

The construction and packaging of the AAV vectors encoding Sig-1R siRNA (AAV-Sig-1R) and control siRNA (AAV-siCon) has been described previously (Tsai et al., 2009). Maps and siRNA sequences are shown in Figure S2.

Cell Culture and Transfection

Mouse neuroblastoma × rat glioma hybrid NG108-15 cells were cultured at 37°C and 5% CO_2 in Dulbecco's modified Eagle's medium (DMEM, Invitrogen) without sodium pyruvate containing 10% fetal bovine serum, 0.1 mM hypoxanthine, 400 nM aminopterin, 0.016 mM thymidine. Mouse neuroblastoma Neuro-2a cells were cultured at 37°C and 5% CO_2 in Minimum Essential Medium (MEM, Invitrogen) containing 10% fetal bovine serum, 100 μg/ml streptomycin sulfate, and 100 U/ml penicillin G sodium. Transfection of cells with expression vectors was done by using PolyJet DNA In Vitro Transfection Reagent (Signagen Laboratories) according to manufacturer's instructions.

Western Blotting

NAc medial shell tissue was microdissected for western blotting following electrophysiological recordings from mice that were infused with AAV-siRNA. See Extended Experimental Procedures for details.

Immunoprecipitation

NAc medial shell was collected using the same procedure as described in Slice Preparation and Solutions, except that slices were transferred to ice-cold ACSF for microdissection and stored on ice until frozen at −80°C. Brain tissues (NAc medial shell combining four or five brains/frontal cortices) were microdissected for immunoprecipitation assays. See Extended Experimental Procedures for details.

Statistics

On >90% of recording days, data were collected from both saline ± BD1063 or cocaine ± BD1063 groups in semirandomized manner. Results are presented as mean ± SEM. Statistical significance was assessed using two-tailed Student's t tests, 1-way ANOVA, or 2-way repeated-measures ANOVA and Bonferroni post hoc tests when appropriate.

SUPPLEMENTAL INFORMATION

Supplemental Information includes Extended Experimental Procedures and seven figures and can be found with this article online at http://dx.doi.org/10.1016/j.cell.2012.12.004.

ACKNOWLEDGMENTS

We thank Drs. Billy T. Chen, Beate C. Finger, and Roy A. Wise for careful reading of the manuscript. We thank Dhara V. Patel, Stephanie Goddard, Janice Joo, and Keenan Hope for technical help. This work was supported by the Intramural Research Program at the National Institute on Drug Abuse. Viral vectors provided by the NIDA Optogenetics and Transgenic Technology Core facility (Lab head: Brandon K. Harvey).

Received: April 16, 2012
Revised: October 5, 2012
Accepted: November 21, 2012
Published: January 17, 2013

REFERENCES

Anderson, S.M., Famous, K.R., Sadri-Vakili, G., Kumaresan, V., Schmidt, H.D., Bass, C.E., Terwilliger, E.F., Cha, J.H., and Pierce, R.C. (2008). CaMKII: a biochemical bridge linking accumbens dopamine and glutamate systems in cocaine seeking. Nat. Neurosci. *11*, 344–353.

Aydar, E., Palmer, C.P., Klyachko, V.A., and Jackson, M.B. (2002). The sigma receptor as a ligand-regulated auxiliary potassium channel subunit. Neuron *34*, 399–410.

Carlezon, W.A., Jr., and Thomas, M.J. (2009). Biological substrates of reward and aversion: a nucleus accumbens activity hypothesis. Neuropharmacology *56*(*Suppl 1*), 122–132.

Chen, Y., Hajipour, A.R., Sievert, M.K., Arbabian, M., and Ruoho, A.E. (2007). Characterization of the cocaine binding site on the sigma-1 receptor. Biochemistry *46*, 3532–3542.

Crottès, D., Martial, S., Rapetti-Mauss, R., Pisani, D.F., Loriol, C., Pellissier, B., Martin, P., Chevet, E., Borgese, F., and Soriani, O. (2011). Sig1R protein regulates hERG channel expression through a post-translational mechanism in leukemic cells. J. Biol. Chem. *286*, 27947–27958.

Dong, L.Y., Cheng, Z.X., Fu, Y.M., Wang, Z.M., Zhu, Y.H., Sun, J.L., Dong, Y., and Zheng, P. (2007). Neurosteroid dehydroepiandrosterone sulfate enhances spontaneous glutamate release in rat prelimbic cortex through activation of dopamine D1 and sigma-1 receptor. Neuropharmacology *52*, 966–974.

Gundlach, A.L., Largent, B.L., and Snyder, S.H. (1986). Autoradiographic localization of sigma receptor binding sites in guinea pig and rat central nervous system with (+)3H-3-(3-hydroxyphenyl)-N-(1-propyl)piperidine. J. Neurosci. *6*, 1757–1770.

Hayashi, T., and Su, T.P. (2001). Regulating ankyrin dynamics: roles of sigma-1 receptors. Proc. Natl. Acad. Sci. USA *98*, 491–496.

Hayashi, T., and Su, T.P. (2003). Intracellular dynamics of sigma-1 receptors (sigma(1) binding sites) in NG108-15 cells. J. Pharmacol. Exp. Ther. *306*, 726–733.

Hayashi, T., and Su, T.P. (2007). Sigma-1 receptor chaperones at the ER-mitochondrion interface regulate Ca(2+) signaling and cell survival. Cell *131*, 596–610.

He, Y.L., Zhang, C.L., Gao, X.F., Yao, J.J., Hu, C.L., and Mei, Y.A. (2012). Cyproheptadine enhances the I(K) of mouse cortical neurons through sigma-1 receptor-mediated intracellular signal pathway. PLoS ONE *7*, e41303.

Hille, B. (2001). Ionic Channels of Excitable Membranes, Third Edition (Sunderland, MA: Sinauer Associates).

Hopf, F.W., Cascini, M.G., Gordon, A.S., Diamond, I., and Bonci, A. (2003). Cooperative activation of dopamine D1 and D2 receptors increases spike firing of nucleus accumbens neurons via G-protein betagamma subunits. J. Neurosci. *23*, 5079–5087.

Hu, X.T., Basu, S., and White, F.J. (2004). Repeated cocaine administration suppresses HVA-Ca2+ potentials and enhances activity of K+ channels in rat nucleus accumbens neurons. J. Neurophysiol. *92*, 1597–1607.

Ikemoto, S. (2010). Brain reward circuitry beyond the mesolimbic dopamine system: a neurobiological theory. Neurosci. Biobehav. Rev. *35*, 129–150.

Ishikawa, M., Mu, P., Moyer, J.T., Wolf, J.A., Quock, R.M., Davies, N.M., Hu, X.T., Schlüter, O.M., and Dong, Y. (2009). Homeostatic synapse-driven membrane plasticity in nucleus accumbens neurons. J. Neurosci. *29*, 5820–5831.

Johannessen, M., Ramachandran, S., Riemer, L., Ramos-Serrano, A., Ruoho, A.E., and Jackson, M.B. (2009). Voltage-gated sodium channel modulation by sigma-receptors in cardiac myocytes and heterologous systems. Am. J. Physiol. Cell Physiol. *296*, C1049–C1057.

Kahoun, J.R., and Ruoho, A.E. (1992). (125I)iodoazidococaine, a photoaffinity label for the haloperidol-sensitive sigma receptor. Proc. Natl. Acad. Sci. USA *89*, 1393–1397.

Kelley, A.E. (2004). Ventral striatal control of appetitive motivation: role in ingestive behavior and reward-related learning. Neurosci. Biobehav. Rev. *27*, 765–776.

Kinoshita, M., Matsuoka, Y., Suzuki, T., Mirrielees, J., and Yang, J. (2012). Sigma-1 receptor alters the kinetics of Kv1.3 voltage gated potassium channels but not the sensitivity to receptor ligands. Brain Res. *1452*, 1–9.

Kourrich, S., and Thomas, M.J. (2009). Similar neurons, opposite adaptations: psychostimulant experience differentially alters firing properties in accumbens core versus shell. J. Neurosci. *29*, 12275–12283.

Kourrich, S., Klug, J.R., Mayford, M., and Thomas, M.J. (2012a). AMPAR-independent effect of striatal αCaMKII promotes the sensitization of cocaine reward. J. Neurosci. *32*, 6578–6586.

Kourrich, S., Su, T.P., Fujimoto, M., and Bonci, A. (2012b). The sigma-1 receptor: roles in neuronal plasticity and disease. Trends Neurosci. *35*, 762–771. http://dx.doi.org/10.1016/j.tins.2012.1009.1007.

Krause, M., German, P.W., Taha, S.A., and Fields, H.L. (2010). A pause in nucleus accumbens neuron firing is required to initiate and maintain feeding. J. Neurosci. *30*, 4746–4756.

Lupardus, P.J., Wilke, R.A., Aydar, E., Palmer, C.P., Chen, Y., Ruoho, A.E., and Jackson, M.B. (2000). Membrane-delimited coupling between sigma receptors and K+ channels in rat neurohypophysial terminals requires neither G-protein nor ATP. J. Physiol. *526*, 527–539.

Martina, M., Turcotte, M.E., Halman, S., and Bergeron, R. (2007). The sigma-1 receptor modulates NMDA receptor synaptic transmission and plasticity via SK channels in rat hippocampus. J. Physiol. *578*, 143–157.

Matsumoto, R.R., Bowen, W.D., Tom, M.A., Vo, V.N., Truong, D.D., and De Costa, B.R. (1995). Characterization of two novel sigma receptor ligands: antidystonic effects in rats suggest sigma receptor antagonism. Eur. J. Pharmacol. *280*, 301–310.

Maurice, T., and Su, T.P. (2009). The pharmacology of sigma-1 receptors. Pharmacol. Ther. *124*, 195–206.

Mavlyutov, T.A., Epstein, M.L., Andersen, K.A., Ziskind-Conhaim, L., and Ruoho, A.E. (2010). The sigma-1 receptor is enriched in postsynaptic sites of C-terminals in mouse motoneurons. An anatomical and behavioral study. Neuroscience *167*, 247–255.

Moriguchi, S., Yamamoto, Y., Ikuno, T., and Fukunaga, K. (2011). Sigma-1 receptor stimulation by dehydroepiandrosterone ameliorates cognitive impairment through activation of CaM kinase II, protein kinase C and extracellular signal-regulated kinase in olfactory bulbectomized mice. J. Neurochem. *117*, 879–891.

Mu, P., Moyer, J.T., Ishikawa, M., Zhang, Y., Panksepp, J., Sorg, B.A., Schlüter, O.M., and Dong, Y. (2010). Exposure to cocaine dynamically regulates the intrinsic membrane excitability of nucleus accumbens neurons. J. Neurosci. *30*, 3689–3699.

Navarro, G., Moreno, E., Aymerich, M., Marcellino, D., McCormick, P.J., Mallol, J., Cortés, A., Casadó, V., Canela, E.I., Ortiz, J., et al. (2010). Direct involvement of sigma-1 receptors in the dopamine D1 receptor-mediated effects of cocaine. Proc. Natl. Acad. Sci. USA *107*, 18676–18681.

Nisenbaum, E.S., Xu, Z.C., and Wilson, C.J. (1994). Contribution of a slowly inactivating potassium current to the transition to firing of neostriatal spiny projection neurons. J. Neurophysiol. *71*, 1174–1189.

Paxinos, G., and Franklin, K.B.J. (2001). The mouse brain in stereotaxic coordinates (Amsterdam: Elsevier Academic).

Perez, M.F., White, F.J., and Hu, X.T. (2006). Dopamine D(2) receptor modulation of K(+) channel activity regulates excitability of nucleus accumbens neurons at different membrane potentials. J. Neurophysiol. *96*, 2217–2228.

Reynolds, S.M., and Berridge, K.C. (2002). Positive and negative motivation in nucleus accumbens shell: bivalent rostrocaudal gradients for GABA-elicited eating, taste "liking"/"disliking" reactions, place preference/avoidance, and fear. J. Neurosci. *22*, 7308–7320.

Robinson, T.E., and Berridge, K.C. (2008). Review. The incentive sensitization theory of addiction: some current issues. Philos. Trans. R. Soc. Lond. B Biol. Sci. *363*, 3137–3146.

Shen, W., Hernandez-Lopez, S., Tkatch, T., Held, J.E., and Surmeier, D.J. (2004). Kv1.2-containing K+ channels regulate subthreshold excitability of striatal medium spiny neurons. J. Neurophysiol. *91*, 1337–1349.

Soriani, O., Vaudry, H., Mei, Y.A., Roman, F., and Cazin, L. (1998). Sigma ligands stimulate the electrical activity of frog pituitary melanotrope cells through a G-protein-dependent inhibition of potassium conductances. J. Pharmacol. Exp. Ther. *286*, 163–171.

Stewart, J. (2004). Pathways to relapse: factors controlling the reinitiation of drug seeking after abstinence. Nebr. Symp. Motiv. *50*, 197–234.

Stocker, M. (2004). Ca(2+)-activated K+ channels: molecular determinants and function of the SK family. Nat. Rev. Neurosci. *5*, 758–770.

Su, T.P., Hayashi, T., Maurice, T., Buch, S., and Ruoho, A.E. (2010). The sigma-1 receptor chaperone as an inter-organelle signaling modulator. Trends Pharmacol. Sci. *31*, 557–566.

Taha, S.A., and Fields, H.L. (2006). Inhibitions of nucleus accumbens neurons encode a gating signal for reward-directed behavior. J. Neurosci. *26*, 217–222.

Tsai, S.Y., Hayashi, T., Harvey, B.K., Wang, Y., Wu, W.W., Shen, R.F., Zhang, Y., Becker, K.G., Hoffer, B.J., and Su, T.P. (2009). Sigma-1 receptors regulate hippocampal dendritic spine formation via a free radical-sensitive mechanism involving Rac1xGTP pathway. Proc. Natl. Acad. Sci. USA *106*, 22468–22473.

Vacher, H., Mohapatra, D.P., and Trimmer, J.S. (2008). Localization and targeting of voltage-dependent ion channels in mammalian central neurons. Physiol. Rev. *88*, 1407–1447.

Varga, A.W., Anderson, A.E., Adams, J.P., Vogel, H., and Sweatt, J.D. (2000). Input-specific immunolocalization of differentially phosphorylated Kv4.2 in the mouse brain. Learn. Mem. *7*, 321–332.

Varga, A.W., Yuan, L.L., Anderson, A.E., Schrader, L.A., Wu, G.Y., Gatchel, J.R., Johnston, D., and Sweatt, J.D. (2004). Calcium-calmodulin-dependent kinase II modulates Kv4.2 channel expression and upregulates neuronal A-type potassium currents. J. Neurosci. *24*, 3643–3654.

Zhang, H., and Cuevas, J. (2005). sigma Receptor activation blocks potassium channels and depresses neuroexcitability in rat intracardiac neurons. J. Pharmacol. Exp. Ther. *313*, 1387–1396.